Acta Derm Venereol (Stockh) 1998; 78: 402–407

Differential Epidermal Expression of the Invariant Chain in Allergic and Irritant Contact Dermatitis

AXEL EMILSON[1], MAGNUS LINDBERG[2] and ANNIKA SCHEYNIUS[1]

[1]Department of Laboratory Medicine, Division of Clinical Immunology, Karolinska Institute and Hospital, Stockholm and [2]Department of Dermatology, University Hospital, Uppsala, Sweden

Allergic contact dermatitis and irritant contact dermatitis have different pathogenic mechanisms. It is therefore plausible that the epidermal expression of HLA-DR and the invariant chain associated with antigen processing and presentation might differ between allergic contact dermatitis and irritant contact dermatitis. We have quantified the volume of epidermal HLA-DR and invariant chain reactivity and the total epidermal volume in allergic contact dermatitis and irritant contact dermatitis using confocal laser scanning microscopy and indirect immunofluorescence on acetone-fixed 25 μm thick vertical skin sections. Eight nickel allergic patients were patch-tested with 5% nickel sulfate and 8 healthy volunteers were patch-tested with 4% sodium lauryl sulfate. Skin biopsy specimens were taken at 0, 6, 24, and 72 h after application of the patch tests. Sodium lauryl sulfate induced a statistically significant increased epidermal volume at 24 h and 72 h compared to 0 h and 6 h ($p < 0.003$ and $p < 0.001$, respectively), whereas an increase in epidermal volume in the allergic contact dermatitis group was not noted until 72 h after patch testing with nickel sulfate compared to 0, 6 h ($p < 0.001$) and 24 h ($p < 0.004$). No significant changes in the epidermal volume of HLA-DR reactivity were found at any time point within or between the two groups, nor was there any significant change in the epidermal volume of invariant chain reactivity in the allergic contact dermatitis group. In the irritant contact dermatitis group, however, the epidermal volume of invariant chain reactivity was significantly reduced from $17 \pm 8 \times 10^3$ μm^3 at 24 h to $9 \pm 3 \times 10^3$ μm^3 at 72 h ($p < 0.04$), which was also significantly lower than the $14 \pm 4 \times 10^3$ μm^3 observed in allergic contact dermatitis at 72 h ($p < 0.01$). Furthermore, the invariant chain expression was significantly lower than the HLA-DR reactivity in the irritant contact dermatitis group at 72 h ($p < 0.001$). The decrease of invariant chain reactivity at 72 h in irritant contact dermatitis might reflect an epitope-induced alteration by sodium lauryl sulfate or a down-regulated biosynthesis of the invariant chain due to variance in local cytokine production between allergic contact dermatitis and irritant contact dermatitis.
Key words: human skin; Langerhans' cell; confocal microscopy.

(Accepted April 20, 1998.)

Acta Derm Venereol (Stockh) 1998; 78: 402–407.

Annika Scheynius, Department of Laboratory Medicine, Division of Clinical Immunology, Karolinska Hospital, S-171 76 Stockholm, Sweden.

Different pathogenic mechanisms are involved in allergic contact dermatitis (ACD) and irritant contact dermatitis (ICD) (1). Although knowledge of the cellular and molecular events in ACD is expanding (2–4), the detailed mechanisms are still not completely understood.

An allergic contact reaction requires an antigen-presenting cell. The dominating antigen-presenting cells in the epidermis are the Langerhans' cells (LCs), which constitutively express the MHC class II molecules and the invariant chain (CD74) (5, 6). Recent studies have underlined the importance of the invariant chain in antigen processing, i.e. the formation of MHC class II peptide complexes, in both murine (7) and human (8) antigen-presenting cells. The invariant chain associates with MHC class II molecules in the endoplasmic reticulum, directs the intracellular transport of MHC class II molecules and prevents premature peptide loading of MHC class II molecules. Peptides from degraded endocytosed proteins or self proteins are finally supposed to meet the MHC class II invariant chain complex in specialized vesicular structures, so-called MHC class II compartments (MIICs) (8–10). In the MIICs, removal of the class II associated invariant chain peptide region (CLIP) of the invariant chain from the peptide binding groove, allows peptide loading of MHC class II molecules and subsequent transport to the cell surface for presentation (8). The removal of CLIP requires the presence of HLA-DM, a non-polymorphic class II molecule, which influences the exchange of peptides bound to class II molecules (8, 11).

Although ACD and ICD have different pathogenic mechanisms, the two conditions can be indistinguishable at the clinical and histological levels (1). The cell infiltrates have been reported to be almost identical in ACD and ICD with a dominance of CD4+ T-lymphocytes (12–14), whereas conflicting data have been found regarding the number of LCs (12, 15, 16). Recently, cytokine expression has been found to differ between ACD and ICD. The upregulation of IL-1β in LCs seems to be highly specific for the induction phase of ACD but not ICD in both human (17) and murine systems (18, 19).

Since no specific immunologic mechanism is supposed to be involved in ICD, it is plausible that the expression of MHC class II and the invariant chain might differ between ACD and ICD. In the present study we have quantified the volume of epidermal HLA-DR and invariant chain reactivity and the total epidermal volume at different time points in ACD and ICD using confocal laser scanning microscopy (CLSM). CLSM is a technique based on point illumination and point detection with suppression of out-of-focus light, which yields improved resolution, especially in the vertical dimension, and which permits optical sectioning (20). All data are digitally stored, thus allowing subsequent image analysis and three-dimensional (3-D) reconstruction (20, 21). Due to the optical sectioning capacity of CLSM, it is possible to investigate a relatively thick tissue specimen and obtain large measurement volumes (22, 23).

MATERIAL AND METHODS

Subjects

Eight patients, all women, aged 20–53 years (median 39 years), with established contact sensitivity to nickel, but otherwise healthy, and 8

 ISSN 0001-5555

healthy volunteers, 4 men and 4 women, aged 23–58 years (median 31 years) with no clinical or anamnestic signs of skin diseases or atopy participated in the study. The study was approved by the Ethics Committee at the University Hospital of Uppsala, and all participants gave their informed consent.

Epicutaneous patch tests

The test substances were applied under occlusion in three Finn Chambers (Epitest Ltd., Oy, Helsinki, Finland), diameter 8 mm, on the gluteal area in order to test non-sun-exposed skin. Allergic reactions were elicited with 5% nickel sulfate (Chemo Technique, Malmö, Sweden) in petrolatum in the ACD group, and irritative reactions were evoked with 4% sodium lauryl sulfate (SLS, Henckel-Niopco AB, Gothenburg, Sweden) in distilled water (w/v) in the ICD group. The three Finn Chambers were removed after 6, 24 and 48 h, respectively. The skin response to the patch tests was graded visually at the time of biopsy using a scale from 0–3, where 0 = no reaction, 0.5 = erythema, 1 = erythema with oedema, 2 = erythema, oedema and papules and 3 = erythema, oedema and vesiculation.

Skin biopsy specimens

Punch biopsies (4 mm) were taken after intradermal injection of local anaesthetic (Lidocaine, Astra, Sweden) from the central part of each patch test skin site and from non-occluded skin in each participant. The specimens were obtained immediately after 6 and 24 h of occlusion and at 24 h after removal of the 48 h of occlusion, i.e. 72 h after test application. For each person, all skin biopsies were taken at the same time. The biopsies were immediately snap-frozen in chilled isopentane and stored at $-70^{\circ}C$ until cryosectioned.

Histological evaluations

Two vertical cryostat sections, 6 μm thick, from each skin biopsy specimen were fixed in acetone and processed for routine hematoxylin and eosin staining. In addition to qualitative assessment of each biopsy, a somewhat modified version of a previously described semi-quantitative method (14) was used to score the allergic and irritant responses under coded conditions by one investigator (AE).

Indirect immunofluorescence staining

Vertical cryostat sections, 25 μm thick, stored at $-70^{\circ}C$, were taken from storage and immediately fixed at 4°C in 50% (w/v) acetone for 30 s followed by 5 min in 100% acetone, and were thereafter allowed to dry for 5 min at 22°C (room temperature). The sections were washed in phosphate-buffered saline (PBS) and incubated with a mouse monoclonal antibody (MoAb) against HLA-DR αβ (clone L243, IgG_{2ak}, diluted 1/100, Becton Dickinson, Sunnyvale, CA, USA), or a mouse MoAb recognizing the invariant chain associated to HLA-DR (MAB1291, IgG_1, diluted 1/20, Chemicon Int., Temecula, CA, USA) for 30 min at room temperature in a humidity chamber. After new washes in PBS, the sections were allowed to react with the secondary antibody, fluorescein-isothiocyanate (FITC) conjugated rabbit anti-mouse IgG (F(ab′)2), diluted 1/20, (Dakopatts, Copenhagen, Denmark) for another 30 min at room temperature. The sections were finally washed in PBS before they were mounted with glycerol in PBS containing 0.5% para-phenylenediamine to reduce fading of immunofluorescence during microscopy (24). Specificity tests included omission of the primary MoAbs or replacement with normal mouse serum. Staining was not observed in these tests. For technical reasons, the control skin biopsy specimen in one patient in the ACD group and the skin biopsy specimen taken at 72 h in one individual in the ICD group were not available for IIF staining and CLSM analysis.

Confocal laser scanning microscopy (CLSM)

The 25 μm thick vertical cryosections were analysed using a SARASTRO® 2000 CLSM beam scanning system (Molecular Dynamics, Sunnyvale, CA, USA) built around a Nikon Optiphot II upright microscope and an argon ion laser. For detection of FITC, the 488 nm laser wavelength was used together with a 510 nm dichroic beamsplitter, reflecting light <510 nm, a 50 μm confocal aperture and a 510 nm long-pass filter in front of the detector, i.e. a photomultiplier tube. The laser power at the laser head aperture was 15 mW. The laser light was attenuated by use of a neutral density filter (30% transmission). The photomultiplier tube-voltage was adjusted so that the full scale of the 8-bit signal digitization (256 gray levels) was utilized, i.e. avoiding both compression and saturation of the dynamic range of the signal in each experiment. To allow comparison among the images obtained, the photomultiplier tube setting was not adjusted between recordings of different optical images within the same experiment. The software for scanning and processing the data, Imagespace (Molecular Dynamics) was implemented on a Personal Iris 25/4D computer (Silicon Graphics, Mountainview, CA, USA). The software compensated for the difference in refractive index of the immersion medium (air = 1.0) and the embedding medium (PPD in glycerol = 1.4), which would affect the depth scale of the analysed volume (25).

Stereological measurements with CLSM

The examination was performed under coded conditions by one investigator (AE). For both antibodies (L243 and MAB1291), two vertical sections from each biopsy specimen from each individual were stained and investigated for stereological measurements on the same occasion. The examination was performed with a $\times 40/0.95$ plano apochromate Nikon objective and a $\times 10$ eye piece. The picture element (pixel) size used for all measurements was 0.5×0.5 μm; the picture size was 512×512 pixels (256×256 μm^2). On each of the two skin sections, the third and fifth fields of view from the left side of the skin section were chosen. When hair follicles or epidermal disruption in the epidermis was present in the field of view, the specimen was moved one field of view in the predefined direction. In each field of view, a stack of six optical sections was scanned, thus giving a total of 24 optical sections per skin biopsy. The scan time for each optical section was approximately 7 s. The optical sections in each stack were scanned with a z-increment of 1.5 μm, starting 3.0 μm from the top surface of the skin section. For each vertical skin section, the penetration of the antibodies was examined with vertical z-scans. The vertical scan was also used to determine the z co-ordinate of the top surface on each skin section. The start position for the horizontal scanning of optical sections was determined by this vertical scan. In addition to the stereological measurements on each skin biopsy, a morphological assessment of the indirect immunofluorescence-stained sections was performed by ocular observation. Morphological features of the stained LCs were assessed: cell morphology, position in the epidermis and pattern of intracellular staining.

Image processing

Each optical stack was evaluated using the Imagespace software as previously described (23). In brief, individual threshold data of each optical stack were processed using an algorithm (26). From each optical stack, an extended focus projection was calculated. An extended focus projection is a 2-D representation of 3-D data. All optical sections in the optical stack are added together, producing the extended focus projection where all sections are in focus. By using extended focus projections, the basal membrane of the epidermis was well visualized, giving a suitable map of the epidermis. A map of the epidermis, excluding the stratum corneum, was drawn for each extended focus projection (one for each stack of 6 optical sections). The mean size ($\pm$SD) of the user drawn maps was $82{,}528 \pm 30{,}458$ pixels ($n = 240$ maps, range 30,441–210,544 pixels). In each stack, the area of pixels of intensity greater than the algorithm-indicated threshold in each image was determined. A mean volume was calculated for each optical stack (mean of 6 sections), as were the two vertical skin sections for each biopsy specimen (mean of 24 sections, i.e. 4 stacks corresponding to 4 extended focus projections).

Statistics

The histopathological features and the skin reactions at different patch test times were analysed with the non-parametric Friedman two-way

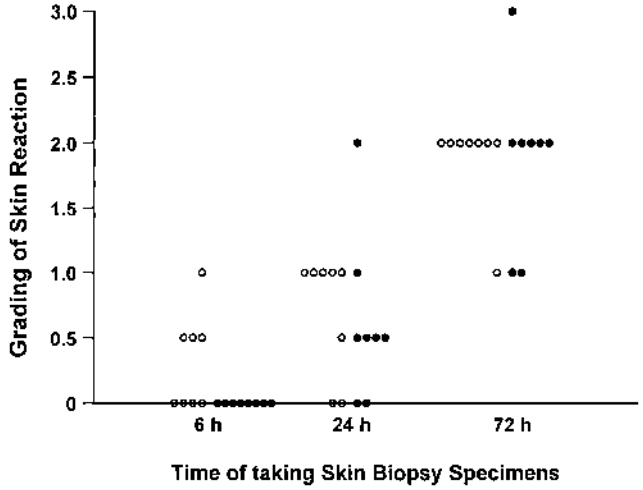

Fig. 1. The ocular evaluation of the skin reactions at the time of taking skin biopsy specimens. In both the ICD (○) and ACD groups (●), a significantly increased skin reaction score was found at 72 h compared to 6 h ($p<0.05$ and $p<0.01$, respectively; $n=8$). 0 = no reaction, 0.5 = erythema, 1 = erythema with oedema, 2 = erythema, oedema and papules, and 3 = erythema, oedema and vesiculation.

analysis of variance (ANOVA) using Prostat version 1.04 for Windows 95® (Poly Software, Salt Lake City, UT, USA). The epidermal volume of HLA-DR and invariant chain reactivity and the total measured epidermal volume at different patch test times compared to those measured in non-occluded skin and between the ACD group and the ICD group were analysed using a three-way ANOVA with repeated measures on two factors. The factors were as follows: (i) group with two levels, ACD and ICD, (ii) reactivity with the two levels, HLA-DR and invariant chain, and (iii) time with the four time points 0, 6, 24, and 72 h. For the variable epidermal volume of HLA-DR or invariant chain reactivity, the reactivity × group interaction and reactivity × time interaction were significant: $F(1, 14)=11.2$, $p<0.005$ and $F(3, 37)=3.26$, $p<0.05$, respectively. Due to the significant interactions, separate two-way ANOVA with repeated measures on two factors were then applied for the two reactivities (HLA-DR and invariant chain).

In case of significant interaction between group and time, simple effects were examined, i.e. effects of one factor holding the other factor fixed. The missing data with CLSM at 0 h from one individual in the ACD group and from one individual at 72 h in the ICD group were replaced by estimates derived from a regression type procedure (BMDP, Program AM; description and estimation of missing data, Statistical Software, Inc., Los Angeles, CA, USA). The degrees of freedom in the ANOVA for MS_{error} for the time and time × group effects have been reduced by the number of the estimated missing observations. The mean and standard deviation tend to be proportional for the epidermal volume of HLA-DR or invariant chain reactivity and the total measured epidermal volume. Therefore, the variables were log-transformed in order to meet the requirements for an adequate ANOVA. A p-value <0.05 was considered to be statistically significant.

RESULTS

Clinical and histological assessment

There were no signs of skin reaction at the sites where control non-occluded skin biopsy specimens were taken in any of the 16 individuals participating in the study. In both the ICD and ACD groups, there was a significant increase in visual skin reaction score at 72 h after patch testing compared to non-occluded skin ($p<0.01$) and to the score at 6 h ($p<0.05$ and $p<0.01$, respectively; Fig. 1). There were no significant differences in visual score between the two groups at any time point. Hematoxylin and eosin-stained sections from the obtained biopsy specimens were evaluated. There were no significant differences between the two groups at any time point.

Epidermal volume

In the ICD group, a statistically significant increase in epidermal volume as measured with CLSM was found at 24 h and 72 h compared to 0 h and 6 h ($p<0.003$ and $p<0.001$, respectively; Table I) after SLS application. In the ACD group, a significantly larger epidermal volume was not obtained until after 72 h ($p<0.001$ compared to 0 h and 6 h, and $p<0.004$ compared to 24 h; Table I). There was no statistically significant

Table I. *The epidermal volume of HLA-DR reactivity or invariant chain reactivity and the measured epidermal volume with CLSM at different patch test times of ACD and ICD. The figures show mean ± SD ($n=8$).*

Time of taking skin biopsy specimens	Measured epidermal volume ± SD (10^3 μm^3)[a]		Epidermal volume above threshold ± SD (10^3 μm^3)[b]			
			HLA-DR		Invariant chain	
	ACD	ICD	ACD[c]	ICD[c]	ACD	ICD
0 h	147 ± 27	164 ± 39	9 ± 3	16 ± 6	11 ± 4	13 ± 4
6 h	158 ± 20	155 ± 40	11 ± 3	14 ± 5	10 ± 5	11 ± 2
24 h	157 ± 38	222 ± 85[d]	9 ± 2	25 ± 13	11 ± 4	17 ± 8
72 h	238 ± 58[e]	247 ± 49[f]	17 ± 6	22 ± 17[g]	14 ± 4	9 ± 3[h]

[a] For each individual, 4 different epidermal maps in 4 different fields of view were drawn (see MATERIAL AND METHODS).
[b] The mean number of voxels (volume elements) over a chosen threshold on an arbitrary intensity scale (range 0–255) in user-defined maps, corresponding to HLA-DR or invariant chain reactivity, are indicated. Six optical sections in 4 different fields of view per individual were scanned at magnification ×400.
[c] The epidermal volume of HLA-DR reactivity was overall statistically significantly larger in the ICD group compared to the ACD group: $p<0.001$, $n=16$.
[d] $p<0.003$ compared to 0 h and 6 h in the ICD group ($n=8$).
[e] $p<0.001$ compared to 0 h and 6 h and <0.004 compared to 24 h in the ACD group ($n=8$).
[f] $p<0.001$ compared to 0 h and 6 h in the ICD group ($n=8$).
[g] $p<0.001$ compared to the epidermal volume of invariant chain reactivity at 72 h in the ICD group ($n=8$).
[h] $p<0.04$ compared to invariant chain reactivity at 24 h in the ICD group ($n=8$) and <0.01 compared to 72 h in the ACD group ($n=16$).

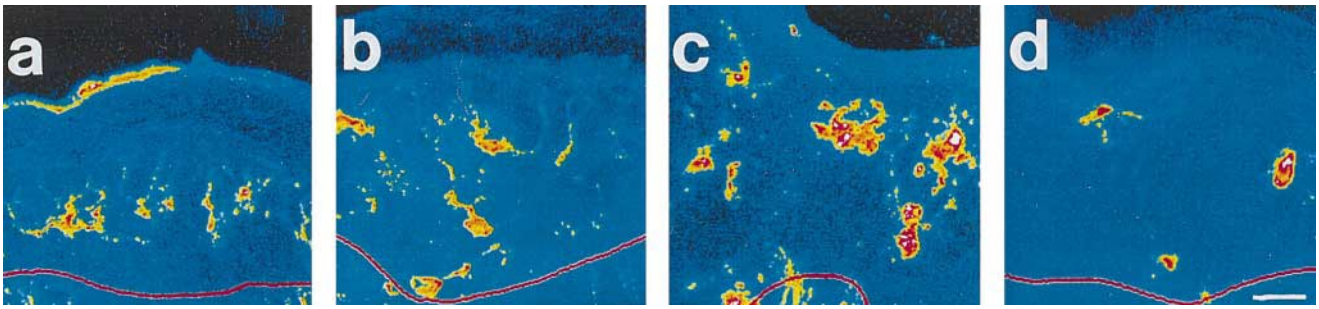

Fig. 2. Three-dimensional reconstructions of LCs from control non-occluded skin (a, b) and from skin 72 h after occlusion for 48 h with 4% SLS in a Finn Chamber® (c, d) in the same individual from the ICD group. Acetone-fixed 25-μm thick vertical sections were incubated with mouse MoAb against HLA-DR (a, c) or the invariant chain (b, d) followed by secondary FITC-conjugated rabbit anti mouse IgG, and analysed with CLSM. The extended focus projections (summation of optical sections in the stack with each section in focus) express the information using a pseudocolour scale (range: white-red-green-blue-black) indicating the strength of the fluorescence intensity, where white is the strongest. Note the changed distribution and cell morphology at 72 h after 48 h occlusion with 4% SLS for both HLA-DR+ (c) and invariant chain+ cells (d) compared to non-occluded skin (a, b). The strong staining in the stratum corneum in (a) represents autofluorescence. The basal membrane of the epidermis is indicated with a red line. The stratum corneum is located at the top in all photos. Size bar = 20 μm.

difference in the epidermal volume at any time point (0–72 h) between the two groups (Table I).

HLA-DR and invariant chain reactivity in the epidermis

The epidermal volume of invariant chain reactivity in non-occluded skin was $11 \pm 4 \times 10^3$ μm^3 in the ACD group and $13 \pm 4 \times 10^3$ μm^3 in the ICD group. No significant change in invariant chain reactivity was found in the ACD group at any time point (Table I). In contrast, SLS induced a significantly decreased invariant chain reactivity at 72 h compared to 24 h in the ICD group ($p < 0.04$, Table I). The invariant chain reactivity at 72 h was significantly lower in the ICD group compared to that in the ACD group ($p < 0.01$, Table I). The epidermal volume of HLA-DR reactivity in non-occluded skin was $9 \pm 3 \times 10^3$ μm^3 in the ACD group and $16 \pm 6 \times 10^3$ μm^3 in the ICD group. There was no significant difference in the epidermal volume of HLA-DR reactivity at any time point (0–72 h) in or between the two groups (Table I). However, there was overall a statistically significantly larger epidermal volume of HLA-DR reactivity in the ICD group compared to the ACD group ($p < 0.001$, Table I).

When comparing the epidermal volume of HLA-DR with that of the invariant chain, we found no significant difference in the ACD group at any time point (0–72 h). In the ICD group, however, the invariant chain reactivity at 72 h was significantly lower compared to the HLA-DR reactivity at 72 h ($p < 0.001$, Table I).

In both the ACD and ICD groups, the HLA-DR+ cells were distributed mainly in the basal and the suprabasal positions of the epidermis at 0 h (Fig. 2a) and 6 h; in a few instances they had a more widespread distribution at 24 h. The distribution of the HLA-DR+ cells shifted toward the basal membrane or the upper the epidermis at 72 h (Fig. 2c). Morphological changes, e.g. rounded/oval HLA-DR+ cells with few and short dendrites were found in 4 individuals at 24 h and in 7 individuals at 72 h in the ICD group (Fig. 2c) and in 1 patient at 24 h and in 4 patients at 72 h in the ACD group. Intracellular staining of HLA-DR in one or a few vesicles in HLA-DR+ cells was found in the majority of biopsies (0–72 h) in both groups. HLA-DR expression on keratinocytes was found in only one subject at 72 h in the ACD group, and that epidermal area was not included in the analysis.

The distribution of invariant chain+ cells, the spatial configuration of dendrites and intracellular staining of the invariant chain in vesicles were, in general, similar to those for HLA-DR+ cells. However, in several subjects, the dendrite staining of invariant chain+ cells appeared thinner compared to that of HLA-DR+ cells. Also, the number of dendrites per invariant chain+ cell was somewhat lower than that in HLA-DR+ cells at 72 h in the ICD group (Fig. 2).

DISCUSSION

In the present study, we have used immunofluorescence, together with CLSM, to measure the epidermal volume of HLA-DR and invariant chain reactivity and the total epidermal volume in biopsy specimens from ACD and ICD at 6, 24, and 72 h after patch testing. The visual grading of the skin reactions gave scores of the same magnitude in ACD and ICD and correlated well with the histopathological findings in the biopsy specimens. Thus, our estimates of the epidermal expression of HLA-DR and the invariant chain in ACD and ICD were performed on clinically comparable skin reactions.

This is, to our knowledge, the first time the epidermal volume in ACD and ICD has been quantified with CLSM. The epidermal volume was significantly increased already 24 h after SLS application in the ICD group, whereas in the ACD group, a statistically significant increase in epidermal volume was not registered until after 72 h. The different kinetics in the increase of epidermal volume in ICD compared to ACD could be due to a direct and more rapid effect of SLS on the epidermal milieu (27). No significant changes in the epidermal volume of HLA-DR reactivity were found at any time point in or between the two groups. Nor was there any significant change in the epidermal volume of invariant chain reactivity in the ACD group. In contrast, we observed a statistically significant reduction in the epidermal volume of invariant chain reactivity in the ICD group at 72 h compared with 24 h, and compared with that in the ACD group at 72 h. The invariant chain expression was also significantly lower than the HLA-DR reactivity at 72 h in the ICD group (Table I). These observed differences between ICD and ACD can reflect a

down-regulated biosynthesis of the invariant chain, but not of HLA-DR in the ICD reaction, due to differences in local cytokine production in these two conditions (19). It has been reported that the levels of MHC class II antigens and the invariant chain in various mouse tissues are differentially regulated in response to cytokines such as IFN-γ (28, 29). SLS might also induce destruction or alteration of the epitope for the used MoAb MAB 1291. Another possibility is that LCs, other antigen-presenting cells, T-cells and various inflammatory cells differ in number due to migration to and from the epidermis (15, 16), and that they differ in their expression of HLA-DR and the invariant chain (30) between ICD and ACD. One must also bear in mind that the MAB 1291 only recognizes the invariant chain when bound to HLA-DR (personal communication, Chemicon Int.).

The finding of an overall significantly larger expression of HLA-DR reactivity in ICD compared to ACD is intriguing. The binding of MoAb L243, used in the present study, is conformation-sensitive (31, 32), and studies indicate that its epitope is involved in peptide binding or T-cell-recognition (33). Thus, the L243 MoAb might not bind to HLA-DR molecules which have the peptide binding groove occupied with self peptides or the invariant chain (32). Additionally, nickel sulfate might interact with peptides bound to HLA-DR (34, 35) and thus induce conformational changes inhibiting binding of L243. It is therefore tempting to speculate that our finding of an overall lower epidermal volume of HLA-DR reactivity in ACD compared to ICD might correspond to differences in the number of conformationally changed HLA-DR molecules, and not to the actual total number of HLA-DR molecules. Perhaps individuals who are prone to develop nickel allergy have a high percentage of self peptide-loaded HLA-DR molecules at the cell surface of antigen-presenting cells, which could yield higher probability for nickel sulfate binding and subsequent T-cell interaction.

The optical sectioning capacity of CLSM allowed us to examine the intracellular distribution of the invariant chain and HLA-DR. Our finding that the invariant chain and HLA-DR accumulated in one or several cytoplasmatic vesicles, probably corresponding to MIICs, agrees with previous studies on human LCs using CLSM or electron microscopy (10, 23).

The relative volume of epidermal HLA-DR reactivity (i.e. epidermal volume of HLA-DR reactivity / measured epidermal volume) for normal non-occluded skin was $7 \pm 2\%$ in the ACD group and $9 \pm 2\%$ in the ICD group. A previous CLSM study of the relative volume of epidermal HLA-DR reactivity in vertical sections of normal human breast skin yielded a mean value of $13 \pm 6\%$ (23). The different values might be explained by variability of LCs density in different body regions, the individual variability of LCs density (36) and different staining protocols. Additionally, the obtained CLSM measures are sensitive for the chosen threshold in the image analysis (37), although the threshold setting is determined from an objective algorithm (26). In the present kinetic study, the epidermal area measured per field of view increased with time and ranged from 30,441 – 210,544 pixels (mean $82{,}528 \pm 30{,}458$ pixels). Significant bias in the CLSM results (e.g. the obtained epidermal volume) due to variations in the measured epidermal area per field of view does not seem plausible, since large numbers of pixels were measured even in the smallest epidermal area (30,441 pixels). Also, HLA-DR expression on keratinocytes does not interfere with our results, since this phenomenon was only found in one individual at 72 h in the ACD group, and this epidermal area was omitted in the analysis. However, some influence from activated epidermal T-cells cannot be completely excluded.

In summary, we found a statistically significant increase in epidermal volume over time in both ICD and ACD. The more rapid increase in epidermal volume in ICD compared to ACD might be due to a direct effect of SLS on the epidermal milieu. There was a significantly reduced epidermal volume of invariant chain reactivity at 72 h compared to 24 h in the ICD group and compared to 72 h in the ACD group. This could point to differences in the biosynthesis rate of the invariant chain between ACD and ICD. Additionally, the epidermal volume of invariant chain reactivity was significantly reduced compared to that of HLA-DR reactivity at 72 h in the ICD. Perhaps different HLA-DR+ cells might express the invariant chain differently, due to varying local epidermal cytokine production in ACD compared with ICD.

ACKNOWLEDGEMENTS

We thank Mrs Anne Svensson for expert technical assistance and MSc Elisabeth Berg and MSc Ulf Brodin, the Department of Medical Information Processing, Karolinska Institute, Stockholm, for valuable help with the statistics. We also thank Assoc Prof Bo Forslind, Experimental Dermatological Research Group, Department of Biophysics, MBB, Karolinska Institute, Stockholm, and PhD Ardan Patwardhan, Department of Laboratory Medicine, Division of Clinical Immunology, Karolinska Hospital, Stockholm, for comments on and discussion of the manuscript. Financial support for this work was received from the Swedish Council for Work Life Research, the Swedish Medical Research Council (grant no. 16X-7924), the Swedish Association against Asthma and Allergy, the Swedish Foundation for Health Care Sciences and Allergy Research, the Hesselman Foundation, and the Welander-Finsen Foundation.

REFERENCES

1. Mozzanica N. Pathogenetic aspects of allergic and irritant contact dermatitis. Clin Dermatol 1992; 10: 115 – 121.
2. Grabbe S, Schwarz T. Immunoregulatory mechanisms involved in elicitation of allergic contact hypersensivity. Am J Contact Dermat 1996; 7: 238 – 246.
3. Katz SI. Dohi Memorial Lecture. The skin as an immunological organ: allergic contact dermatitis as a paradigm. J Dermatol 1993; 20: 593 – 603.
4. Kimber I. Cytokines and regulation of allergic sensitization to chemicals. Toxicology 1994; 93: 1 – 11.
5. Claesson-Welsh L, Scheynius A, Tjernlund U, Peterson PA. Cell surface expression of invariant γ-chain of class II histocompatibility antigens in human skin. J Immunol 1986; 136: 484 – 490.
6. Romani N, Schuler G, Fritsch P. Identification and phenotype of epidermal Langerhans cells. In: Schuler G, ed. Epidermal Langerhans cells. Boca Raton: CRC Press, Inc., 1991: 49 – 86.
7. Elliott EA, Drake JR, Amigorena S, Elsemore J, Webster P, Mellman I, et al. The invariant chain is required for intracellular transport and function of major histocompatibility complex class II molecules. J Exp Med 1994; 179: 681 – 694.
8. Pieters J. MHC class II restricted antigen presentation. Curr Opin Immunol 1997; 9: 89 – 96.
9. Peters PJ, Neefjes JJ, Oorschot V, Ploegh HL, Geuze HJ. Segregation of MHC class II molecules from MHC class I molecules in the Golgi complex for transport to lysosomal compartments. Nature 1991; 349: 669 – 676.
10. Kleijmeer MJ, Oorschot VMJ, Geuze HJ. Human resident Langer-

hans cells display a lysosomal compartment enriched in MHC class II. J Invest Dermatol 1994; 103: 516 – 523.
11. Sloan VS, Cameron P, Porter G, Gammon M, Amaya M, Mellins E, et al. Mediation by HLA-DM of dissociation of peptides from HLA-DR. Nature 1995; 375: 802 – 806.
12. Brasch J, Burgard J, Sterry W. Common pathogenetic pathways in allergic and irritant contact dermatitis. J Invest Dermatol 1992; 98: 166 – 170.
13. Scheynius A, Fischer T, Forsum U, Klareskog L. Phenotypic characterization in situ of inflammatory cells in allergic and irritant contact dermatitis in man. Clin Exp Immunol 1984; 55: 81 – 90.
14. Willis CM, Young E, Brandon DR, Wilkinson JD. Immunopathological and ultrastructural findings in human allergic and irritant contact dermatitis. Br J Dermatol 1986; 115: 305 – 316.
15. Ferguson J, Gibbs J, Swanson Beck J. Lymphocyte subsets and Langerhans cells in allergic and irritant patch test reactions: histometric studies. Contact Dermatitis 1985; 13: 166 – 174.
16. Gerberick GF, Rheins LA, Ryan CA, Ridder GM, Haren M, Miller C, et al. Increases in human epidermal DR+CD1+, DR+CD1 – CD36+, and DR – CD3+ cells in allergic versus irritant patch test responses. J Invest Dermatol 1994; 103: 524 – 529.
17. Rambukkana A, Pistoor FHM, Bos JD, Kapsenberg ML, Das PK. Effects of contact allergens on human Langerhans cells in skin organ culture: migration, modulation of cell surface molecules, and early expression of interleukin-1 β protein. Lab Invest 1996; 74: 422 – 436.
18. Enk AH, Katz SI. Early molecular events in the induction phase of contact sensitivity. Proc Natl Acad Sci USA 1992; 89: 1398 – 1402.
19. Müller G, Knop J, Enk AH. Is cytokine expression responsible for differences between allergens and irritants? Am J Contact Dermatitis 1996; 7: 177 – 184.
20. Wilson T. Confocal microscopy. In: Wilson T, ed. Confocal microscopy. London: Academic Press, 1990: 1 – 60.
21. Scheynius A, Lundahl P. Three-dimensional visualization of human Langerhans cells using confocal scanning laser microscopy. Arch Dermatol Res 1990; 281: 521 – 525.
22. Bergfelt L, Emilson A, Lindberg M, Scheynius A. Quantitative and three-dimensional analysis of Langerhans cells in basal cell carcinoma. A comparative study using light microscopy and confocal laser scanning microscopy. Br J Dermatol 1994; 130: 273 – 280.
23. Emilson A, Scheynius A. Quantitative and three-dimensional analysis of human Langerhans cells in epidermal sheets and vertical skin sections. J Histochem Cytochem 1995; 43: 993 – 998.
24. Johnson GD, Davidson RS, McNamee KC, Russell G, Goodwin D, Holborow EJ. Fading of immunofluorescence during microscopy: a study of the phenomenon and its remedy. J Immunol Methods 1982; 55: 231 – 242.
25. Carlsson K. The influence of specimen refractive index, detector signal integration, and non-uniform scan speed on the imaging properties in confocal microscopy. J Microsc 1991; 163: 167 – 178.
26. Mossberg K, Arvidsson U, Ulfhake B. Computerized quantification of immunofluorescence-labelled axon terminals and analysis of co-localization of neurochemicals in axon terminals with a confocal scanning laser microscope. J Histochem Cytochem 1990; 38: 179 – 190.
27. Fisher LB, Maibach HI. Effect of some irritants on human epidermal mitosis. Contact Dermatitis 1975; 1: 273 – 276.
28. Lechler R, Aichinger G, Lightstone L. The endogenous pathway of MHC class II antigen presentation. Immunol Rev 1996; 151: 51 – 79.
29. Momburg F, Koch N, Möller P, Moldenhauer G, Butcher GW, Hammerling GJ. Differential expression of Ia and Ia-associated invariant chain in mouse tissues after in vivo treatment with IFN-γ. J Immunol 1986; 136: 940 – 948.
30. Kämpgen E, Koch N, Koch F, Stöger P, Heufler C, Schuler G, et al. Class II major histocompatibility complex molecules of murine dendritic cells: synthesis, sialylation of the invariant chain, and antigen processing capacity are down-regulated upon culture. Proc Natl Acad Sci USA 1991; 88: 3014 – 3018.
31. Salamero J, Le Borgnes R, Saudrais C, Goud B, Hoflack B. Expression of major histocompatibility complex class II molecules in HeLA cells promotes the recruitment of ap-1 golgi-specific assembly proteins on golgi membranes. J Biol Chem 1996; 271: 30318 – 30330.
32. Newcomb JR, Carboy-Newcomb C, Cresswell P. Trimeric interactions of the invariant chain and its association with major histocompatibility complex class II αβ dimers. J Biol Chem 1996; 271: 24249 – 24256.
33. Nygard NR, Bono C, Brown LR, Gorka J, Giacoletto KS, Schaiff WT, et al. Antibody recognition of an immunogenic influenza hemaglutinin – human leukocyte antigen class II complex. J Exp Med 1991; 174: 243 – 251.
34. Romagnoli P, Labhardt AM, Sinigaglia F. Selective interaction of Ni with an MHC-bound peptide. EMBO J 1991; 10: 1303 – 1306.
35. Weltzien HU, Moulon C, Martin S, Padovan E, Hartmann U, Kohler J. T-cell immune responses to haptens. Structural models for allergic and autoimmune reactions. Toxicology 1996; 107: 141 – 151.
36. Breathnach SM. Origin, cell lineage, ontogeny, tissue distribution, and kinetics of Langerhans cells. In: Schuler G, ed. Epidermal Langerhans cells. Boca Raton: CRC Press, Inc., 1991: 23 – 47.
37. Scheynius A, Dalenbring M, Carlsson K, England R, Lindberg M. Quantitative analysis of Langerhans cells in the epidermis at irritant contact reactions using confocal laser scanning microscopy. Acta Derm Venereol (Stockh) 1992; 72: 348 – 351.